

RESEARCH

Open Access



Deletion at an 1q24 locus reveals a critical role of long noncoding RNA *DNM3OS* in skeletal development

Ting-ting Yu¹, Qiu-fan Xu^{1†}, Si-Yang Li^{1†}, Hui-jie Huang¹, Sarah Dugan², Lei Shao¹, Jennifer A. Roggenbuck³, Xiao-tong Liu¹, Huai-ze Liu¹, Betsy A. Hirsch⁴, Shen Yue^{1*}, Chen Liu^{1*} and Steven Y. Cheng^{1*}

Abstract

Background: Skeletal development and maintenance are complex processes known to be coordinated by multiple genetic and epigenetic signaling pathways. However, the role of long non-coding RNAs (lncRNAs), a class of crucial epigenetic regulatory molecules, has been under explored in skeletal biology.

Results: Here we report a young patient with short stature, hypothalamic dysfunction and mild macrocephaly, who carries a maternally inherited 690 kb deletion at Chr.1q24.2 encompassing a noncoding RNA gene, *DNM3OS*, embedded on the opposite strand in an intron of the *DYNAMIN 3* (*DNM3*) gene. We show that lncRNA *DNM3OS* sustains the proliferation of chondrocytes independent of two co-cistronic microRNAs *miR-199a* and *miR-214*. We further show that nerve growth factor (*NGF*), a known factor of chondrocyte growth, is a key target of *DNM3OS*-mediated control of chondrocyte proliferation.

Conclusions: This work demonstrates that *DNM3OS* is essential for preventing premature differentiation of chondrocytes required for bone growth through endochondral ossification.

Keywords: Skeletal abnormalities, 1q24, lncRNA, *DNM3OS*, Nerve growth factor

Background

Development of the skeletal system that supports body structures and maintenance of its homeostatic state are highly complex processes orchestrated by an elaborate array of gene activities. A frequently occurring developmental skeletal abnormality is short stature, which can arise as part of systemic diseases [1–3]. Height gain as the result of bone elongation is driven by chondrogenesis occurring at the growth plate, which is a cartilaginous structure located near the ends of weight-bearing bones

in children [4]. Thus, reduced chondrogenesis at growth plates is the main cause underlying short stature.

The rate of chondrogenesis at growth plates depends on several factors, including nutritional intake, systemic hormonal levels, as well as paracrine growth factors and the extracellular matrix signaling [4–7]. Consequently, genetic lesions that disrupt the regulation of in these systems will result in short stature. In fact, genetic testing of children with abnormal growth has identified multiple intracellular pathways that involved in chondrocyte differentiation in the growth plate. One of them is the *RAS* oncogene and the mitogen-activated protein kinase (*MAPK*) signaling pathway, which integrate signals from several growth factors such as growth hormone (*GH*), fibroblast growth factors (*FGFs*) and epithelial growth factor (*EGF*) [8–11]. Mutations in this pathway underpin a number of genetic syndromes that are collectively termed ‘rasopathies’; these

*Correspondence: yueshen@njmu.edu.cn; liuchen@njmu.edu.cn; sycheng@njmu.edu.cn

[†]Qiu-fan Xu and Si-Yang Li contributed equally to this work

¹ Department of Medical Genetics, School of Basic Medical Sciences, Nanjing Medical University, Jiangsu 211166 Nanjing, P. R. China
Full list of author information is available at the end of the article



© The Author(s) 2021. This article is licensed under a Creative Commons Attribution 4.0 International License, which permits use, sharing, adaptation, distribution and reproduction in any medium or format, as long as you give appropriate credit to the original author(s) and the source, provide a link to the Creative Commons licence, and indicate if changes were made. The images or other third party material in this article are included in the article's Creative Commons licence, unless indicated otherwise in a credit line to the material. If material is not included in the article's Creative Commons licence and your intended use is not permitted by statutory regulation or exceeds the permitted use, you will need to obtain permission directly from the copyright holder. To view a copy of this licence, visit <http://creativecommons.org/licenses/by/4.0/>. The Creative Commons Public Domain Dedication waiver (<http://creativecommons.org/publicdomain/zero/1.0/>) applies to the data made available in this article, unless otherwise stated in a credit line to the data.

include Noonan syndrome, LEOPARD syndrome, Costello syndrome, as well as cardio-facio-cutaneous and neurofibromatosis–Noonan syndrome, a common element of these syndromes is the postnatal growth failure to varying degrees [12].

Since the beginning of the new millennium, mounting evidence has shown that microRNAs and long non-coding RNAs play critical roles in regulating various cellular processes [13]). These non-coding RNAs regulate gene expression and cell signaling through diverse mechanisms. However, while lncRNAs that regulate epigenetic control of gene expression, development as well as govern human traits have been rapidly identified, few lncRNAs have been implicated in skeletal biology. Here, we reported a patient with short stature, hypothalamic dysfunction and mild macrocephaly, who carries a maternally inherited 690 kb deletion at Chr.1q24.2 encompassing a long noncoding RNA gene, *DNM3OS*. This lncRNA reading frame is of 7.8 kb in length embedded on the opposite strand within the 14th intron of the *DYNAMIN 3* gene (*DNM3*), and carries two microRNAs: *miR-199a-5p* and *miR-214*. Our data show that it is capable of promoting primary chondrocyte proliferation and inhibiting chondrocyte differentiation via up-regulating nerve growth factor (*NGF*). Our data further show that the mouse counterpart of this lncRNA, *Dnm3os*, is a bona fide regulatory factor of skeleton development independent of its embedded co-cistronic *miR199a* and *miR214*.

Results

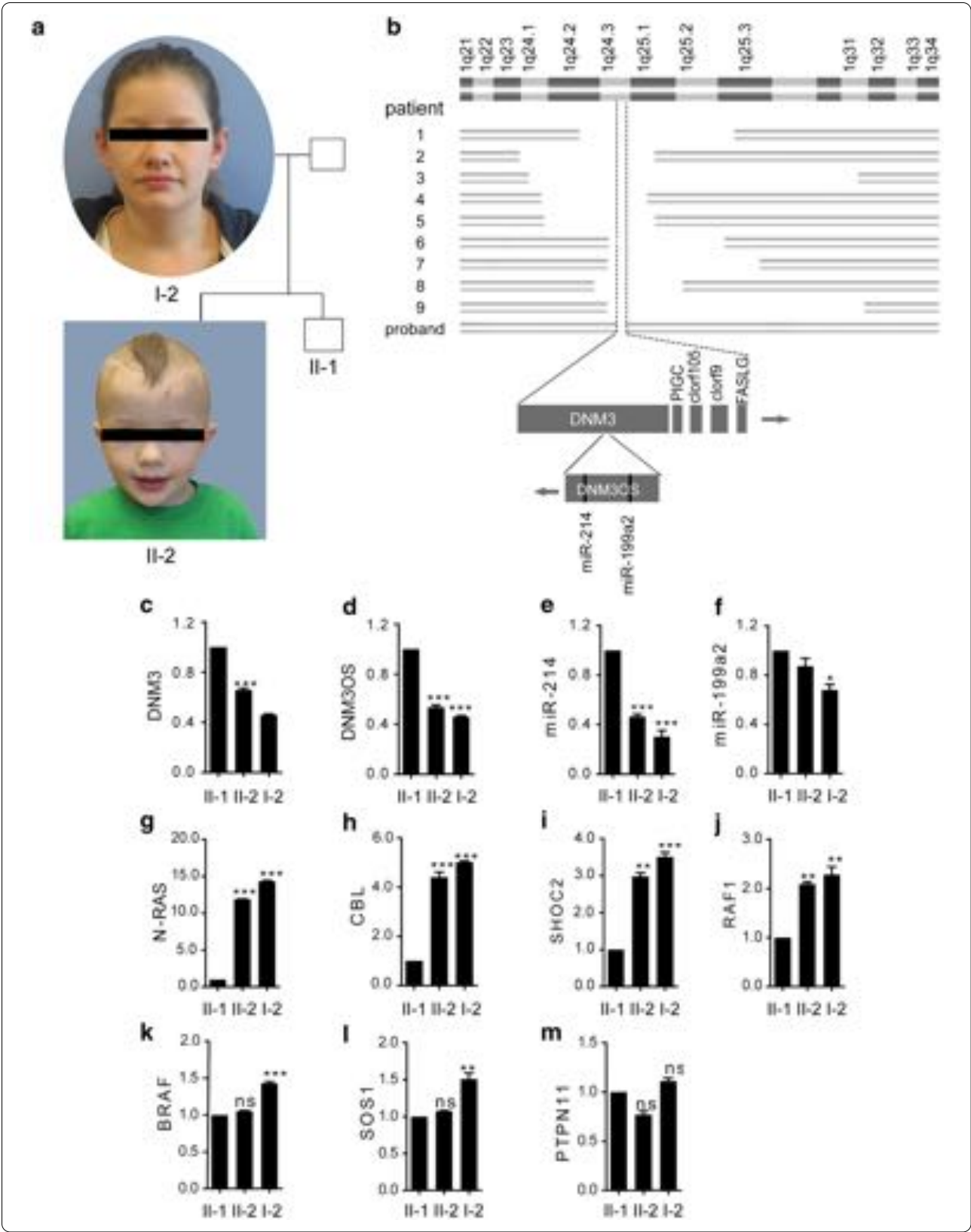
Deletion of *DNM3OS* is associated with developmental delay

A young boy was presented to us with clinical manifestation of short stature, hypothalamic dysfunction and mild macrocephaly reminiscent of Noonan syndrome (Fig. 1a, and Additional file 1). The birth weight and height of the proband (II-2) were both below the 5th percentile among Caucasians, and radiographic examinations first conducted at 2 years of age indicated delayed bone growth; however, laboratory tests found no hormonal imbalance, and tests for mutations in 12 known genes compiled in the Noonan Spectrum Chip were also negative (data not shown). Using oligonucleotide-based array comparative genomic hybridization, we identified a maternally inherited 690 kb deletion at 1q24.3 (Fig. 1b), which falls within the common

chromosomal deletion interval reported in a cohort of 9 patients with facial features, prenatal-onset short stature with delayed bone age, single palmar crease, and brachydactyly similar to the proband [14]. Deletions around 1q24–1q25 have been noted for growth deficiency among a myriad of symptoms [15]. Among 5 protein-coding genes and undefined open reading frames in the deleted region, we were drawn to a transcription unit called *DNM3OS* on the opposite strand in the 14th intron of *DNM3*, which encodes no protein but two microRNAs, *miR-199a-5p* and *miR-214* (Fig. 1b). In the literature, homozygous deletion of murine *Dnm3os* was reported to cause severe skeletal defects in new born mice including cranial deformity, which was most likely the cause of postnatal lethality, but it was not clear whether the long noncoding RNA *Dnm3os* as a whole, or *miR-199a-5p* or *miR-214* plays that essential role for the skeletal development [16]. Previously we demonstrated that *miR-214* down-regulates *N-ras* to promote myogenic differentiation at the expense of osteogenic differentiation [17]; however, genetic ablation of *miR-214* did not lead to obvious signs of Noonan syndrome-like features including growth delay in mice [18, 19] (Additional file 2: Fig. S1). Nevertheless, expression of 7 Noonan syndrome genes in the *Ras* pathway was drastically increased (Additional file 3: Fig. S2) in MEF cells isolated from *miR-214* knock-out mice, in keeping with the presence of *miR-214* recognition sites in the 3'UTR or coding regions of these RNA transcripts (Additional file 4: Table S1). Using real-time PCR, we found that the levels of *DNM3*, *DNM3OS*, and *miR-214* RNA transcripts in the peripheral blood of the proband (II-2) and his carrier mother (I-2) were only 50% of those in his non-carrier brother (II-1) (Fig. 1c–f). Interestingly, the peripheral expression of 4 out of the same 7 Noonan syndrome genes tested in *miR-214* KO mice was significantly increased in carriers II-2 and I-2 relative to the non-carrier II-1 (Fig. 1g–m). These data suggest that *DNM3OS* carries an essential function that accounts for the roles of chromosomal 1q23–1q25 interval in skeletal development and although the ablation of *miR-214* in mice is not sufficient to cause phenotype that resembles any aspect of the partial Noonan syndrome manifestation seen in the proband, it nevertheless partakes in the regulation of skeletal growth via the *Ras* pathway.

(See figure on next page.)

Fig. 1 Deletion of lncRNA-*DNM3OS* is associated with autosomal dominant inheritance of 1q24 deletion syndrome phenotypes. **a** Family tree of the proband (II-2). **b** Chromosomal maps of a cohort of 9 individuals with 1q24–25 deletions. **c–f** RT-qPCR quantifications of *DNM3* mRNA, lncRNA-*DNM3OS*, *miR-214*, and *miR-199* in the blood. The 3' stem-loop primer for human *miR-199* recognizes both *miR-199a* and *miR-199b* on chromosome 9, the latter of which is not affected by the deletion. **g–m** RT-qPCR quantifications of *N-RAS*, *CBL*, *SHOC2*, *RAF1*, *BRAF*, *SOS1*, and *PTPN11* in the blood. One-way ANOVA test was used for statistical analysis. **P < 0.01, ***P < 0.001, and ns, not significant



Murine *Dnm3os* is required for maintaining the proliferative potential of articular chondrocytes

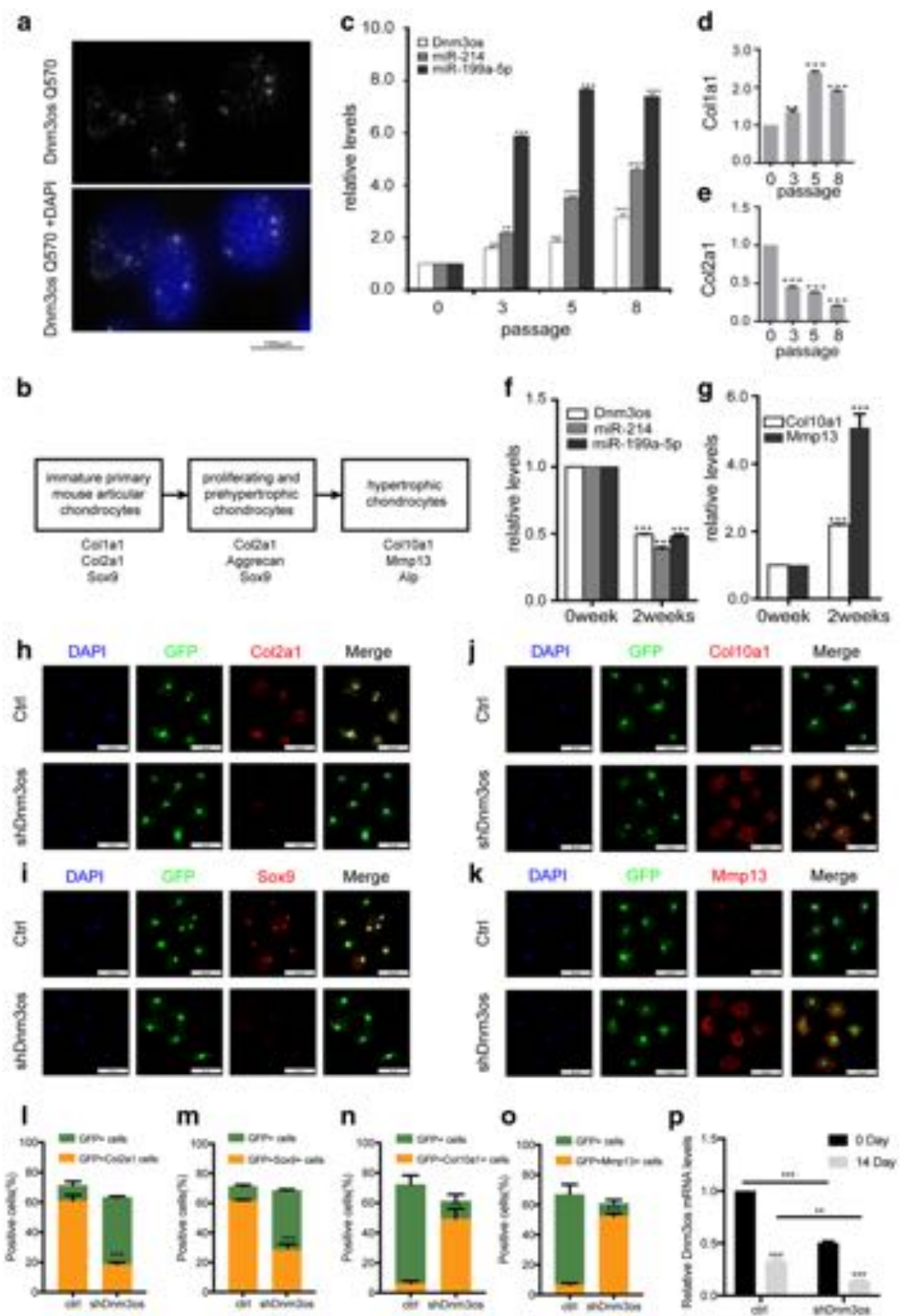
Both human and mouse *Dnm3os* encodes a 7.8 kb RNA transcript, which was identified due to its depleted expression in mouse limb buds lacking basic helix-loop-helix transcription factor *Twist* [20]. First appearing in limb buds and other future skeletal elements [17], robust *Dnm3os* expression was reported in perichondrial cells and periarticular chondrocytes at the cartilage growth plate [16]. Using RNA-FISH, we found that full length *Dnm3os* RNA is confined to the nucleus (Fig. 2a). During embryonic development, chondrocytes in the long bone growth plate undergo an orderly proliferation and differentiation process that eventually gives rise to trabecular bones [21]. This chondrogenic process can be faithfully recapitulated in vitro using isolated immature primary mouse articular chondrocytes (iMAC) [22]. We observed that expression of *Dnm3os* and its co-cistronic *miR-199a-5p* and *miR-214* progressively increased (Fig. 2b, c) following several passages in the maintenance medium as the cells gradually reverted to a “dedifferentiated” state marked by the switch of cell surface collagen types from *Col2a1* to *Col1a1* (Fig. 2d, e). Correspondingly, the expression of chondrogenic transcription factor *SOX9* gradually decreases with passaging (Additional file 5: Fig. S3A). When introducing sh*Dnm3os*, the switch of cell surface collagen types from *Col2a1* to *Col1a1* was slightly slowed, suggesting that *Dnm3os* was not a key fact for dedifferentiated (Additional file 5: Fig. S3B). Conversely, expression levels of these non-coding RNAs all decreased dramatically after the cells were induced to differentiate into hypertrophic chondrocytes marked by *Col10a1* and *MMP13* (Fig. 2f, g). These spatial and temporal expression patterns of *Dnm3os* are consistent with an essential role in promoting the proliferation but suppressing the differentiation of chondrocytes. To ascertain such a function, we silenced *Dnm3os* expression using shRNAs in the iMAC before inducing their differentiation. At the end of two weeks, immunofluorescence microscopy indicated that over 60% of scrambled shRNA transfected cells (marked by GFP) still retained *Col2a1* and *Sox9*, but these percentages

dropped to below 20 and 40%, respectively, in the cells transfected with sh*Dnm3os* (Fig. 2h, i, l, m). Remarkably, many GFP positive cells that received sh*Dnm3os* completely lost *Col2a1* and *Sox9* (Fig. 2h, i, l, m), indicating that they had differentiated further into hypertrophic chondrocytes (Fig. 2b). Elevated expression of *Col10a1* and *Mmp13* confirmed the role of silencing *Dnm3os* in promoting chondrogenic differentiation (Fig. 2j, k, n, o). The expression level of *Dnm3os* maintained at a relative low level in the cells transfected with sh*Dnm3os* (Fig. 2p). Moreover, EdU assay showed *Dnm3os* silencing decreased the proliferation of iMAC by 10% (Additional file 5: Fig. S3 C–E).

In addition to controlling *Ras* pathway genes (Additional file 3: Fig. S2), forced expression of *miR-214* and *miR-199a* blocked chondrogenesis (Additional file 6: Fig. S4A–F) and promoted proliferation (Additional file 6: Fig. S4G–H). Thus, to determine if the large *Dnm3os* is sufficient in regulating chondrogenesis or requires the two co-cistronic microRNAs, we cloned the mouse full length *Dnm3os* (FL) and generated a mutant that lacks both microRNAs (DKO). RT-QPCR analysis confirmed the overexpression of FL and DKO in iMAC cells (Additional file 5: Fig. S3H). Forced expression of either FL or the DKO mutant *Dnm3os* impeded the chondrogenesis as evident by reduced staining by alcian blue (Fig. 3a, b) or of alkaline phosphatase (Fig. 3c, d), which mark the cartilage matrix proteins and the mature hypertrophic chondrocytes, respectively. The effects of DKO in chondrogenesis were not due to the dominant-negative inhibition of endogenous *Dnm3os* function, since overexpression of DKO inhibited chondrogenesis as shown by decreased *Mmp13* and *Col10a1* in iMAC cells silencing endogenous *Dnm3os* with sh*Dnm3os* transfection (Additional file 5: Fig. S3F–G). Forced expression of the DKO mutant also showed similar propensity to down-regulate the same cohort of *Ras* pathway genes as the parental RNA (Additional file 7: Fig. S5), indicating that *Dnm3os* can function independently of the two microRNAs. Finally, to ascertain if *Dnm3os* directly promotes the proliferation of articular chondrocytes, we labeled the cells with EdU and found that both the FL and DKO mutant *Dnm3os* accelerated the cell growth (Fig. 3e, f).

(See figure on next page.)

Fig. 2 LncRNA- *Dnm3os* is required for maintaining the proliferative potential of chondrocytes. **a** RNA-FISH detection of lncRNA-*Dnm3os* in NIH3T3 cells using Quasar 570 labelled Stellaris oligonucleotide probe. **b** Flow chart of in vitro chondrogenic differentiation. **c** RT-qPCR detection of RNAs in primary articular chondrocytes at passages as noted. **d, e** RT-qPCR detection of proliferating chondrocyte marker, *Col2a1*, and osteoblast marker *Col1a1*, respectively; the latter cell descends from mesenchymal lineage. **f** RT-qPCR detection of RNA and **g** hypertrophic chondrocyte markers *Col10a1* and *Mmp13* following differentiation for 2 weeks. **h–k** IF staining of *Col2a1*, *Sox9*, *Col10a1*, and *Mmp13* and **l–o** quantification thereof following differentiation for 2 weeks. Prior to induction of differentiation, the primary articular chondrocytes were transfected with scrambled shRNA (ctrl) or sh*Dnm3os*, both of which carried a GFP marker. **p** RT-qPCR detection of *Dnm3os* at the start and end of in vitro chondrogenic differentiation. Student T-test was used for statistical analysis. **P < 0.01, ***P < 0.001



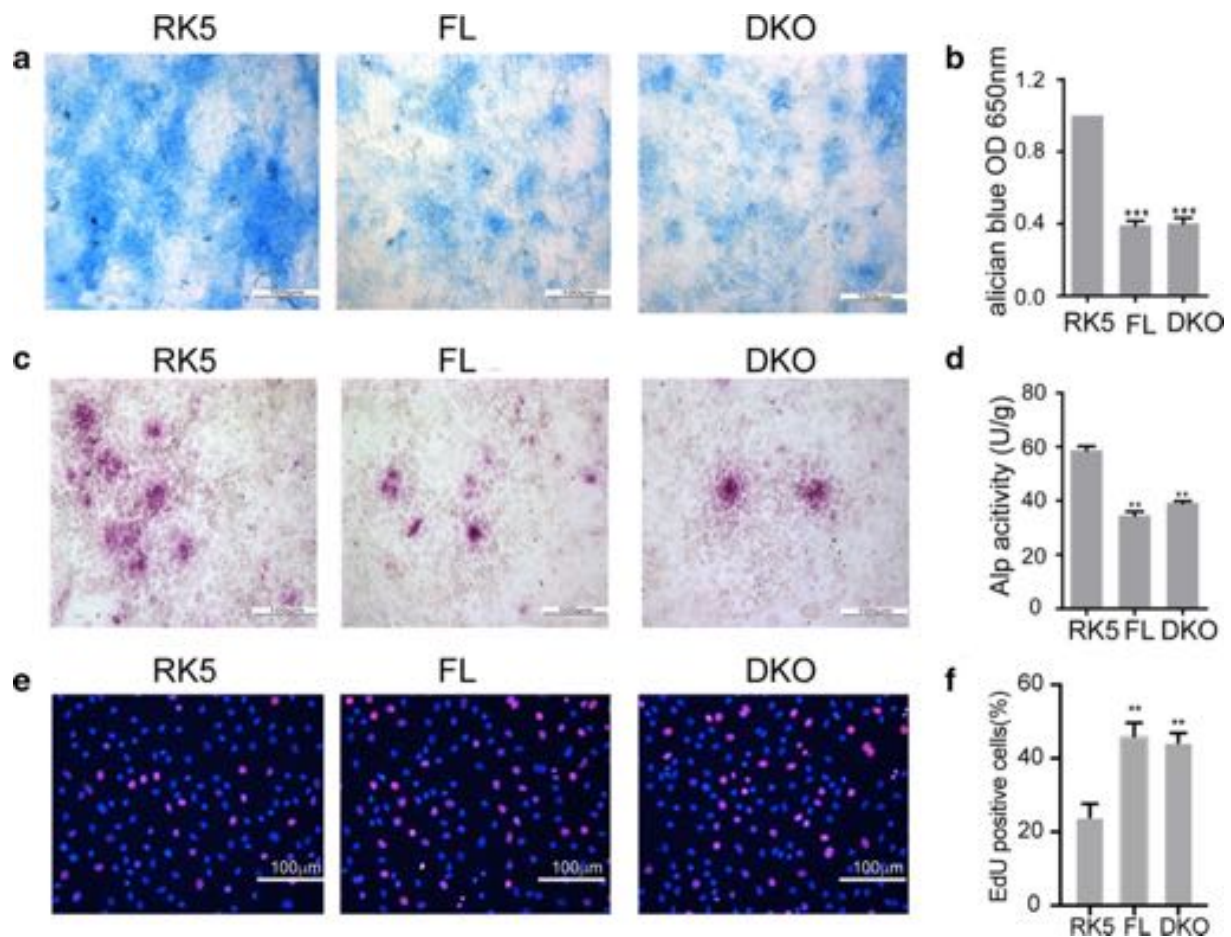


Fig. 3 LncRNA-*Dnm3os* sustains the proliferation of chondrocytes independent of the co-cistronic microRNAs. **a** Alcian blue staining and **b** quantification thereof of cartilage matrix produced by differentiated chondrocytes. **c** Alkaline phosphatase staining and **d** quantification thereof of differentiated chondrocytes. The primary articular chondrocytes were transfected with the control vector or constructs that express FL or the mutant *Dnm3os* prior to induction of chondrogenic differentiation. **e** EdU labeling of proliferating chondrocytes and **f** calculation thereof. The primary articular chondrocytes were transfected as in (a–c), and one day later the cells were labeled with EdU for 8 hours before visualization. The frequency of nuclear EdU labeling is determined by examination of at least three random fields, magnification $\times 400$ and at least 300 cells and nuclei in each group. One-way ANOVA test was used for statistical analysis. ** $P < 0.01$, *** $P < 0.001$

Dnm3os is required for maintaining the proliferative potential of ATDC5 cells

To corroborate the above observation in primary mouse articular chondrocytes, we took the advantage of ATDC5 cells that are widely used as an in vitro model for chondrocyte differentiation to test the pro-proliferative role of *Dnm3os*. Alcian blue staining images collected by light microscopy over an 18-day time-course indicated that insulin-supplemented differentiation medium cultivation successfully induced the differentiation of ATDC5 cells to mature hypertrophic chondrocytes (Additional file 8: Fig. S6A). Decreased *Col2a1* and increased *Col1a1* expression confirmed the differentiation on the biomarker (Additional file 8: Fig. S6B, C). Consistent with primary mouse articular chondrocytes, the expression

of *Dnm3os* in ATDC5 cells gradually decreased with the chondrogenic differentiation (Additional file 8: Fig. S6D). Overexpression of FL and the DKO mutant *Dnm3os* activated ATDC5 cells proliferation and impeded the chondrogenesis as evident by 2-fold increased EDU positive cells (Fig. 4a, b and Additional file 5: Fig. S3I) and absent Alcian blue staining (Fig. 4c), while silencing *Dnm3os* with shRNA inhibited the proliferation of ATDC5 cells (Fig. 4d, e). We further employed RT-QPCR to examined the expression of *Sox9* in FL and DKO transfected ATDC5 cells and iMAC cells. Both overexpression of FL and DKO increased the expression level of *Sox9* in ATDC5 cells, while the effect in iMAC cells were barely observed (Additional file 8: Fig. S6E, F). However, the expression of *Sox9* decreased with iMAC cells passing

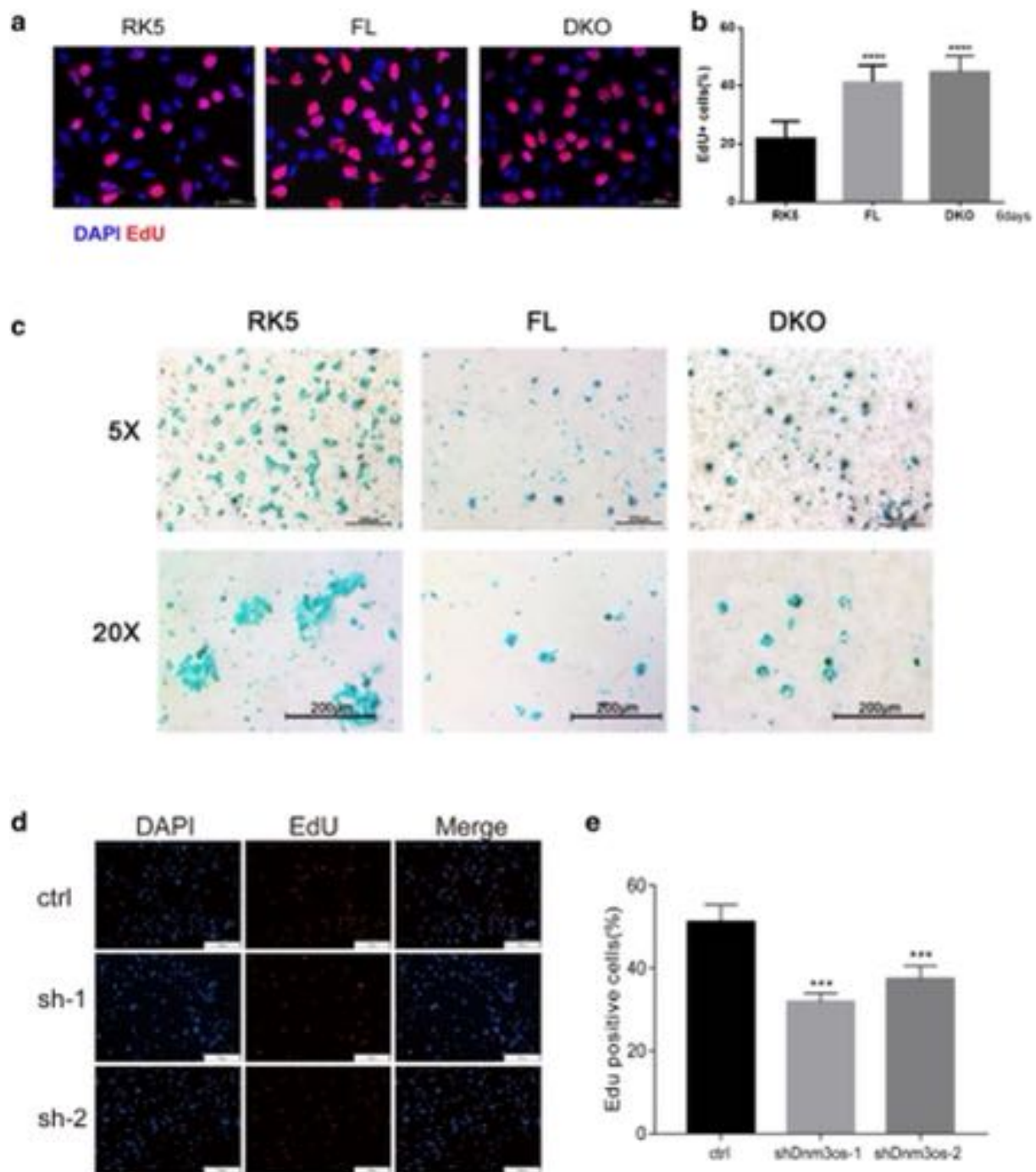


Fig. 4 LncRNA-*Dnm3os* is required for maintaining the proliferative potential of the ATDC5 cells. **a** EdU labeling of proliferating ATDC5 cells and **b** calculation thereof. The ATDC5 cells were transfected by RK5, FL and DKO individually, and one day later the cells were labeled with EdU for 8 hours before visualization. **c** Alcian blue staining of cartilage matrix produced by differentiated ATDC5 cells. **d** EdU labeling of proliferating ATDC5 cells and **e** calculation thereof. The ATDC5 cells were transfected with scrambled shRNA, sh*Dnm3os*-1 and sh*Dnm3os*-2 individually, and one day later the cells were labeled with EdU for 8 h before visualization. The frequency of nuclear EdU labeling in (**a**) and (**d**) were determined by examination of at least three random fields, magnification $\times 400$ and at least 300 cells and nuclei in each group. One-way ANOVA test was used for statistical analysis. *** $P < 0.001$, **** $P < 0.0001$, and ns, not significant

(Additional file 5: Fig. S3A), which suggested the overexpression of FL and DKO to some extent counteracted the reduction of *Sox9* caused by passage. These data suggest that *Dnm3os* contributes to the maintenance of ATDC5 and iMAC cells as chondrogenic progenitors and plays an independent role in regulating chondrogenesis instead of simply acting as a precursor of miRNAs.

***NGF* is a potential *Dnm3os*-regulated gene in chondrocytes**

To substantiate the direct link between *Dnm3os* and chondrogenesis, we performed RNA-seq in FL and DKO mutant *Dnm3os* transfected primary mouse articular chondrocytes with 2 biological replicates. The result showed 250 and 211 differentially expressed genes in FL and DKO overexpressed cells relative to the RK5 transfected control cells, respectively (Fig. 5a), and of these, 155 were commonly expressed in those two cells transfected with *Dnm3os* vectors, suggesting that this lncRNA functions as an independent regulator of chondrocytes (Fig. 5a) and DKO acts as a regulator at the transcriptional level. To predict the biological function of *Dnm3os*, we categorized these 155 genes into defined pathways and we found cell cycle appeared in the top altered pathways, which confirmed the proliferation effect of *Dnm3os* (Additional file 8: Fig. S6G). To further provide biological insight to the differential expression genes, the 155 genes were assigned into defined pathways by using Reactome databases (Fig. 5b). Among the top 20 significantly altered pathways ranked in the dot plot enrichment map, signal transduction, metabolism and extracellular matrix organization, whose dynamics are key to tissue morphogenesis appeared with majority gene enrichment and statistical significance. We further dissected 8 of the top enriched pathways and found matrix metalloproteinase 3, collagen genes including *Col8a2*, *Col23a* and growth factors including *NGF*, *FGF*, as visualized by the heat map (Fig. 5c). The expression changes of these genes suggested the ongoing extracellular matrix remodeling and accelerated cell proliferation. Subsequently, we picked up 14 genes which have been reported to play a role in chondrocyte proliferation or differentiation and verified the change by QPCR analysis (Fig. 5d, e). To exclude the *miR-214* target genes, we detected the expression of these 14

genes in *miR-214* transfected ATDC5 cells simultaneously, and found *NGF* was a potential target gene regulated by lncRNA-*Dnm3os* specifically (Fig. 5e).

***Dnm3os*-induced *NGF* maintains the proliferative potential of ATDC5 cells**

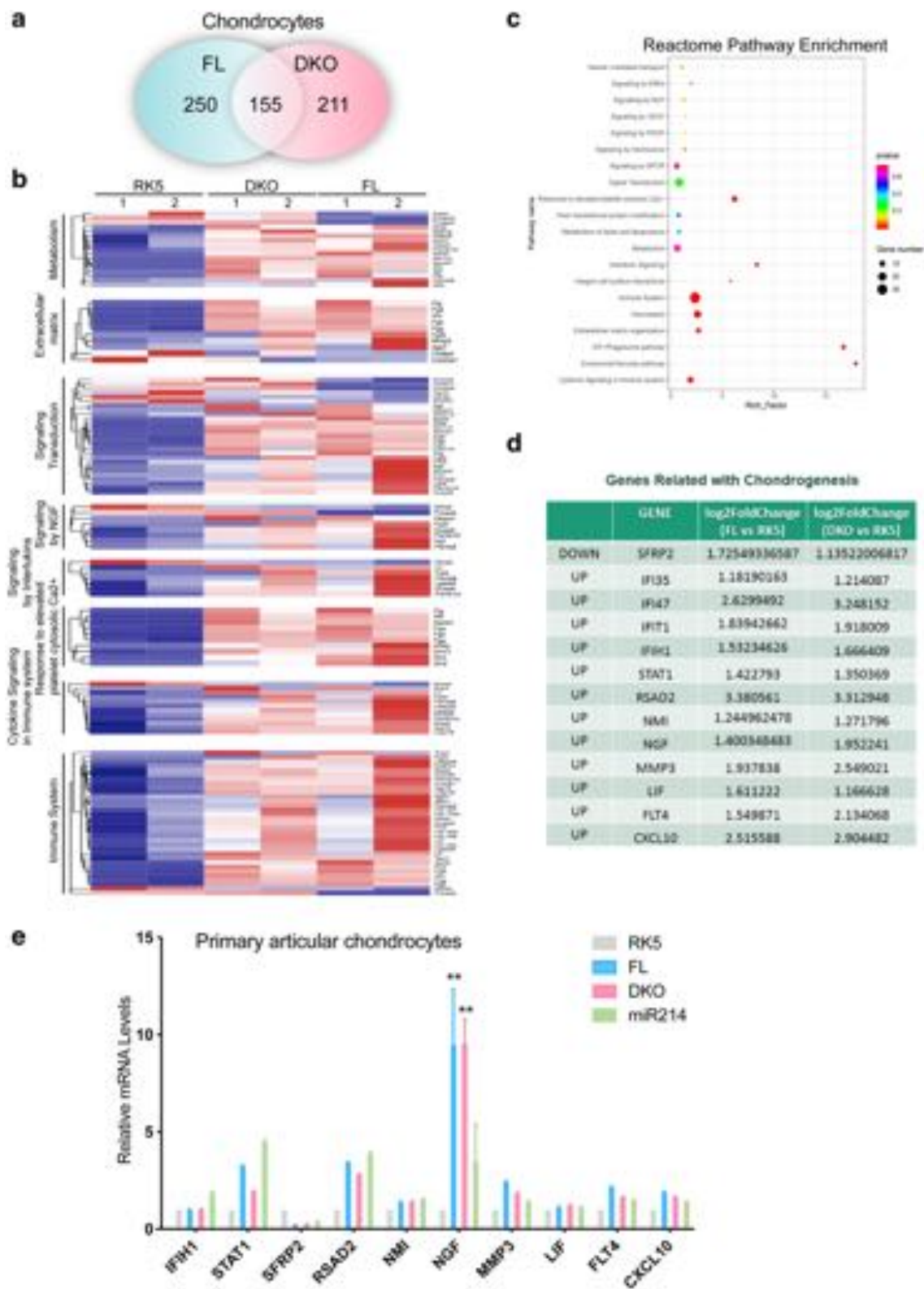
As a neuropeptide, *NGF* was involved in cartilage metabolism and is reported to mediate the chondrogenic differentiation of mesenchymal stem cells [23]. To determine if *NGF* play a role in *Dnm3os* mediated chondrocytes proliferation, we treat FL, DKO mutant and *miR-214* transfected ATDC5 cells with PD90780, an inhibitor of *NGF*. 24 hours after treatment, we labeled the cells with EdU and found that inhibition of *NGF* blocked FL and DKO mutant *Dnm3os*-induced chondrocytes proliferation (Fig. 6a, b). On the other hand, the chondrogenesis was promoted by PD90780 as evident by increased staining by alcian blue in FL and DKO mutant *Dnm3os* transfected cells after 18-days differentiation (Fig. 6c, d). Consistently, FL and DKO mutant *Dnm3os*-induced collagen types switch from *Col1a1* to *Col2a1* was interrupted by PD90780 (Fig. 6e, f). *MMP9*, a target gene of *NGF* was downregulated with treatment of PD90780 and validated the inhibitory effect of the compound (Fig. 6g). RT-QPCR analysis of *Col10a1* confirmed the that inhibition of *NGF* in FL and DKO constructs overexpressing cells promoted differentiation (Fig. 6h). These data collectively indicated these chondrocytes have been released from the bondage of *Dnm3os* and entered the differentiation state.

Discussion

Skeletal development is a complex process that exquisitely controlled both spatially and temporally by cell signaling networks and gene regulation programs. In the past decades, studies of congenital human disease reveal a great deal of genes that involved in bone growth including *Ras-MAPK* pathway, *Wnt* and *Hedgehog* signaling [24, 25]. However, the contribution of non-coding RNA especially lncRNA to skeletal development still remains unclear. Here, we present evidence that shows lncRNA-*Dnm3os* is required for maintaining the proliferative potential of articular chondrocytes, and we demonstrate that *Dnm3os* has specific gene

(See figure on next page.)

Fig. 5 RNA-sequencing analysis of lncRNA-*Dnm3os* regulated genes in chondrogenesis. **a** Quantitative RNA-seq comparison of differentially expressed genes in FL and DKO transfected primary articular chondrocytes. Total number of genes with at least 1.15-log2Fold Change are indicated. **b** Heat map representation of the top 8 enriched pathway with highest fold change in FL and DKO transfected primary articular chondrocytes. **c** Top 20 enriched Reactome pathways in FL and DKO transfected primary articular chondrocytes. The size and color of the dots represent the enriched gene number and the range of p values, respectively. **d** Genes associated with chondrogenesis that are up- or down-regulated in FL and DKO transfected primary articular chondrocytes. **e** Verification of lncRNA-*Dnm3os* regulated genes in **(d)** by RT-qPCR in chondrocytes transfected by RK5, FL, DKO and *miR214* individually. Student T-test was used for statistical analysis. *P < 0.1 and **P < 0.01



targets such as *NGF*, which impeded chondrocytes to differentiation state. Thus, *Dnm3os* defines a new class of lncRNAs that serve as transcriptional regulator in addition to produce microRNAs, thereby forming a regulatory network that maintains a proper pool of proliferating chondrocytes to supply bone growth through endochondral ossification, which account for the short stature.

In 2011, Burkardt et al. reported nine patients with a core clinical symptom of mental retardation, microcephaly accompanied by short stature, and identified a crucial deletion region spanning 1.9 Mb at 1q24.3q25.1 [14]. The deleted region contains 13 genes including *Dynamin 3 (DNM3)* and *CENPL*, which encodes a protein essential for centromeric function, mitotic progression and synaptic reaction. Later, Ashraf T described 2 patients with 1q24 microdeletions and the skeletal phenotype, but had normal intellect or mild learning impairment [26]. Genetic testing of these 2 patients narrows the skeletal abnormalities to a region containing only *DNM3* and a transcript union in the opposite strand of *DNM3*, which called *DNM3* opposite strand (*Dnm3os*). This unit can be transcribed into a long non-coding RNA *Dnm3os* (lncRNA-*Dnm3os*), which was described as a precursor of two microRNAs: *miR-199a-5p* and *miR-214*. It was reported that *Dnm3os*, *miR214* and *miR199a-5p* are abundant in the skeleton system containing limb and skull [27]. *Dnm3os* deletion mice exhibited several skeletal abnormalities, including craniofacial hypoplasia and defects of dorsal neural arches [16]. Down regulation of *miR199a-214* cluster, especially *miR-214* was considered to be responsible of the phenotype. While for quite a long time, lncRNA-*Dnm3os* was described as a precursor of these two miRNAs. However, *miR-214* KO mice were born at Mendelian ratios and displayed a minimal reduction in body weight compared with WT littermates. Our experiments revealed scientific explanations for these paradoxical phenomena. First, lncRNA-*Dnm3os* may have compensatory effect of skeletal development since lncRNA-*Dnm3os* shares most of the target genes with *miR-214*, and genetic deletion of the *miR199a-214* cluster did not abolish the regulatory effect of lncRNA-*Dnm3os* (Figs. 3 and 4). The other possible explanation is lncRNA-*Dnm3os* has its own target genes which

involved in skeletal development. Thus, the *Dnm3os* transcript unit defines a regulatory network between lncRNA and miRNAs.

During the past decades, emerging evidence suggests that lncRNAs can play a crucial role in manipulating various cellular processes. In particular, lncRNAs can serve as master gene regulators at transcriptional and posttranscriptional levels, participating in embryonic development and occurrence of diseases. In some cases, lncRNAs can act as baits of microRNA and sequester microRNA for target mRNAs transcriptional repression. Other lncRNAs including *BACE1 AS* regulate gene expression by competing with miRNAs. And for some lncRNAs, their degradation can be triggered by microRNA. Recently, research works defined the interaction between nucleolin, *ILF-2* and lncRNA-*Dnm3os* by RNA pull-down assays with macrophage nuclear lysates, which indicates that lncRNA-*Dnm3os* is more than a precursor of microRNAs. Due to the obvious and direct link to vertebrate skeleton development, lncRNA-*Dnm3os* may also have unique function in this biological process.

Conclusions

This study demonstrated that lncRNA-*DNM3OS* maintains the proliferation and restrains premature differentiation of chondrocytes independent of the co-cistronic microRNAs *miR-199a* and *miR-214*. In addition, mechanistic studies showed *NGF* as a key target of lncRNA-*DNM3OS* that supports chondrocyte proliferation. Combined with our findings, lncRNA-*DNM3OS* likely plays an important role in regulating skeletal development by triggering *NGF* signaling. Future studies are required to ascertain whether there are more particular genes or signaling pathways regulated by lncRNA-*DNM3OS*.

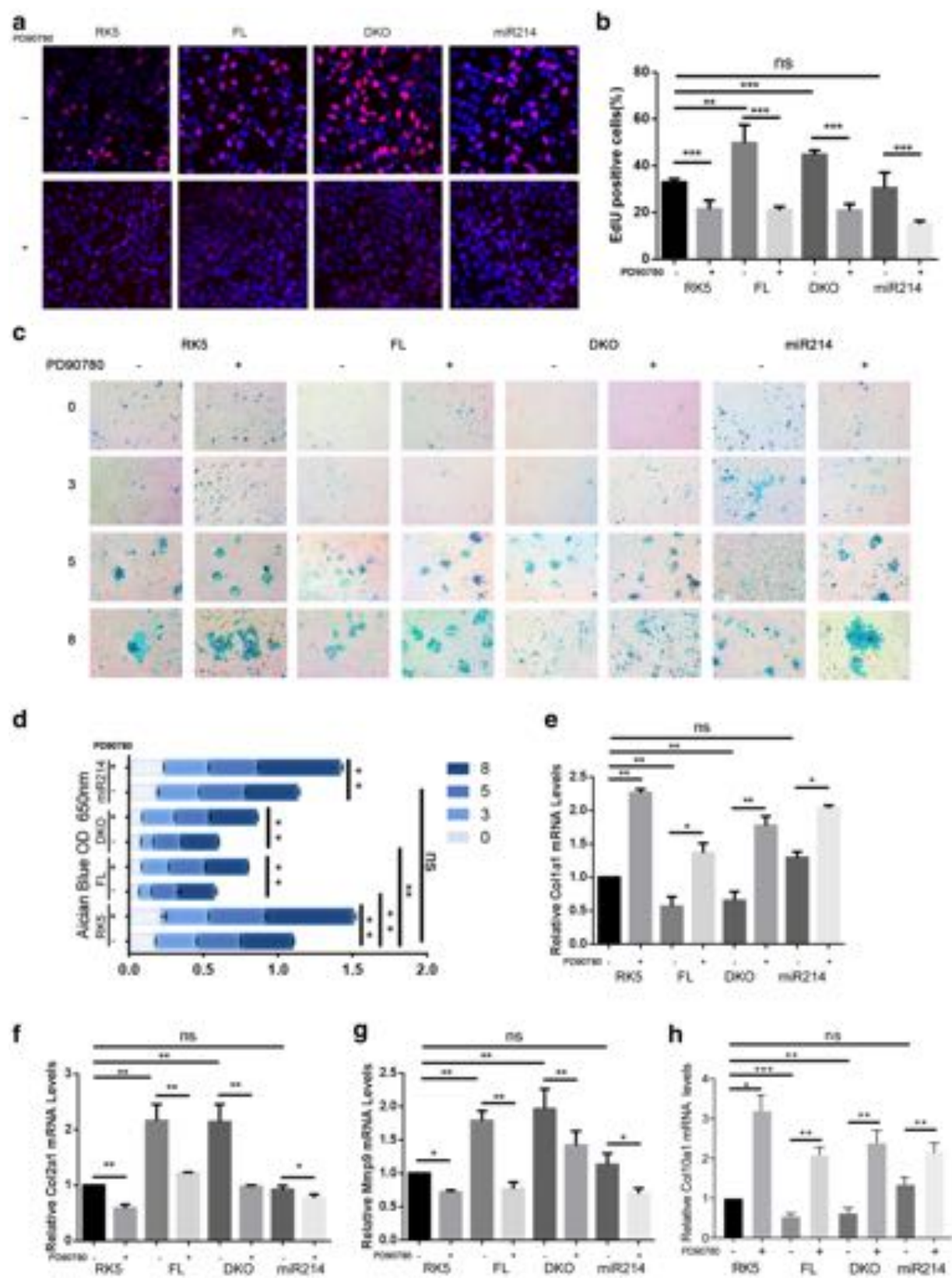
Materials and methods

Single family case studies

The studies of this case obtained the informed consent from all subjects. For publication of photos, consent was obtained from the patients.

(See figure on next page.)

Fig. 6 lncRNA-*Dnm3os* sustains the proliferation of chondrocytes by upregulating *NGF*. **a** EdU labeling of proliferating ATDC5 cells and **b** calculation thereof. The ATDC5 cells transfected by RK5, FL, DKO, and miR214 were treated with vehicle of PD90780 (1% DMSO) or PD90780 (10 µg/1 ml) for 24 hours, and one day later the cells were labeled with EdU for 8 h before visualization. The frequency of nuclear EdU labeling is determined by examination of at least three random fields, magnification ×400 and at least 300 cells and nuclei in each group. **c** Alcian blue staining and **d** quantification thereof of cartilage matrix produced by the differentiated ATDC5 cells. The ATDC5 cells were transfected and treated with PD90780 as in (a). **e–h** RT-qPCR quantifications of *Col1a1*, *Col2a1*, *Mmp9* and *Col10a1* in ATDC5 cells transfected and treated with PD90780 as in (A). Student T-test was used for statistical analysis. *P < 0.1, **P < 0.01, ***P < 0.001, and ns, not significant



Animals

The studies with animals follow the guidelines and ethical regulations. The research program and study protocols were approved by Animal Care and Ethical Committee of Nanjing Medical University (approval number 14,030,111).

Isolation of mouse articular chondrocytes and culture

Primary chondrocytes were isolated from 5 to 6 days old mice as described. Briefly, cartilages from tibial plateaus and femoral condyles were excised and all extraneous soft tissues were removed. To isolate chondrocytes, the cleaned cartilages were digested two consecutive times in cell culture medium with 3 mg/ml collagenase D (Roche, Indianapolis, 11088858001) at 37 °C for 45 min, and then overnight with 0.5 mg/ml collagenase D. The next day, the dislodged cells were passed through a 2 ml Pasteur pipet successively to disperse aggregates, then through a sterile 48- μ m mesh before collected by centrifugation for 10 min at 400 \times g, 20 °C. The cells were plated out at a density of 25 \times 10³/cm². Chondrogenic differentiation was induced by replacing culture medium with DMEM/F12 (1:1) (Gibco, C11330500BT), supplemented with 10% FBS, 1% pen&strep (Gibco, 15140122), 10 μ g/ml insulin, 10 μ g/ml transferrin, and 3 \times 10⁻⁸ M sodium selenite (Sigma, I3146). The differentiation medium was changed every 3 days.

Plasmids construction and cell transfection

The DNA fragment containing full length *Dnm3os* sequence was amplified by PCR from mouse genomic DNA and inserted between the BamHI and SalI sites in the pRK5 vector to generate pRK5-*Dnm3os*. PCR-based deletion strategy was used to generate the *miR-199a-5p* and *miR-214* deletion mutant (DKO). The PCR primers used are as follows.

FL-F: TTCCTGGTCCTAAATTCATTGCCAG
 FL-R: ATAGGAATAAAAATTACAAGTATGAA
 MiR-199a2D-F1: TTCCTGGTCCTAAATTCATTGCCAG
 MiR-199a2-R1: ACAGGATTTTCCACACACCGA
 MiR-199a2D-F2: ACGCCATGGACGGCTGGGGACACA
 MiR-199a2D-R2: ATAGGAATAAAAATTACAAGTATGAA
 MiR-214D-R1: AACCTGAAGGACCCAAG
 MiR-214D-F1: AAAACCTACCCGAAGTAAAG
 Sh*Dnm3os* was designed by using online tools available from . Oligonucleotides (listed in Additional file 9: Table S2) of sh*Dnm3os* were cloned into pRetro-H1G shRNA expression vector. ShRNA with the sense sequence 5'-agatctTTAGTATAGATAATATTT

CtacctgaccataGAAATATTAT CTATACTATTTTgg-tacc-3' which lacks complementary sequences in the human genome, was used as control (scrambled shRNA).

Primary articular chondrocytes were transfected with endotoxin-free plasmid constructs using Lipofectamine (Invitrogen, 11514-015) according to the manufacturer's procedure.

Blood RNA extraction and RT-qPCR

10 ml blood from each subject was drawn with a BD Vacutainer CPT Cell Preparation Tube containing sodium citrate. Lymphocytes and monocytes were separated from the plasma in Ficoll solution (Sigma, F2637). Briefly, the blood samples were diluted with 1:1 sterile PBS, and then carefully poured onto 10 ml Ficoll solution in a 50 ml centrifuge tube (the blood must remain on top, do not mix). The tubes were centrifuged for 20 min at 350 \times g, and lymphocytes and monocytes between plasma and Ficoll layers were harvested using a sterile pipette. The cells were washed twice with PBS, and the RNA was extracted using the RNAiso reagent (Takara, 9109) to template cDNA synthesis using the PrimeScript RT reagent kit (Takara, RR014). SYBR green real-time qPCR reactions (Vazyme, Q111) were carried out on a ABI7500 Real-Time PCR system. The cycling condition was 95°C for 5 minutes, followed by 40 amplification cycles of 95°C, 15 second and 60°C, 1 minute. For each data point, triplicate reactions were carried out and the experiment was repeated three times to assess the statistical significance. RT-qPCR primer sequences are listed as follows.

PCR primers for human genes

h*NRAS*-F: AACAAAGCCCACGAACT
 h*NRAS*-R: TGGCAATCCCATACAA
 h*CBL*-F: CCACTTGCTCGTCTCC
 h*CBL*-R: AACAGTAGTATCCCACATC
 h*BRAF*-F: CCTCATTACCTGGCTCAC
 h*BRAF*-R: TCTCCCAATCATCACTCG
 h*RAF1*-F: GTCACGCTGGAGTGGTTCT
 h*RAF*-R: ACAATACGATGCCATAGGAGT
 h*SHOC2*-F: TTTTGTCCAGGCTTGAGT
 h*SHOC2*-R: CATCTTTGGCATCTTTCC
 h*SOS1*-F: CTTAGGTGGAGGTGAGAA
 h*SOS1*-R: TGGTCCCTGATTAAATAGA
 h*PTPN11*-F: TATCCTCTGAACTGTGCAGATCC
 h*PTPN11*-R: TCTGGCTCTCTCGTACAAGAAAA
 h*DNM3*-F: AATCCGTCCACTAGAACTCTCA
 h*DNM3*-R: GGTCCATACATGCGACTACTCA
 h*DNM3OS*-F: GGTCTCACCCCTGCTTGTTAATCAA
 h*DNM3OS*-R: TCCTGTTGTTACTGGCCCTCATGC

PCR primers for mouse genes

m*Nras*-F: CCTTGACCCGTTTGACACT
 m*Nras*-R: AACCACCTACATACCTACAT
 m*Cbl*-F: AGGGTTTCACCGTCTT

mCbl-R: CTGGGCTGAGTGTAGTTT
mBraf-F: ACCTCGTCACAGTTCTCCT
mBraf-R: TTCTTGGCTTGAAGTTGC
mRaf-F: TCGCTCGGATGCGAGAAT
mRaf1-R: TGAGGAAGGGCTGGAGG
mShoc2-F: TCGCTTTAATCGCATAAC
mShoc2-R: TGAGCTACATCCAGGGTA
mPtpn11-F: GAGGAGTCGATGGCAGTT
mPtpn11-R: CTGAATCTTGATGTGGGTAA
mMmp13-F: GTTGACAGGCTCCGAGAAAT
mMmp13-R: CATCAGGCACTCCACATCTT
mCol10a1-F: AAGGAGTGCCTGGACACAAT
mCol10a1-R: ATGCCTGGGATCTTACAGGT
mSox9-F: CGGAACAGACTCACATCTCTCC
mSox9-R: GCTTGCACGTCGGTTTTGG
mCol1a1-F: GCTCCTCTTAGGGGCCACT
mCol1a1-R: CCACGTCTCACCATTGGGG
mCol2a1-F: GGGTCACAGAGGTTACCCAG
mCol2a1-R: ACCAGGGGAACCACTCTCAC
mDnm3os-F: CAAGGCTCTCACTTGTCTCTG
mDnm3os-R: CAGCTGGAACTGACCAAAAG
mLfi35-F: GTGACCCTGCAAAGTGCCTC
mLfi35-R: TTCAGGTACTGAGAATGGGATCT
mLfi47-F: TCTCCAGAAACCCTCACTGGT
mLfi47-R: TCAGCGGATTCATCTGCTTCG
mLfi1-F: CTGAGATGTCACTTCACATGGAA
mLfi1-R: GTGCATCCCCAATGGGTCT
mLifh1-F: AGATCAACACCTGTGGTAACACC
mLifh1-R: CTCTAGGGCCTCCACGAACA
mStat1-F: TCACAGTGGTTCGAGCTTCAG
mStat1-R: GCAAACGAGACATCATAGGCA
mSfrp2-F: CGTGGGCTCTTCCTCTTCG
mSfrp2-R: ATGTTCTGGTACTCGATGCCG
mRsd2-F: GCAGAGATGGACGATATGAGAGG
mRsd2-R: GCTGAGTGCTGTTCCCATCT
mNmi-F: GCAGAGATGGACGATATGAGAGG
mNmi-R: CGACTGCAATTCAGCTTCAAGTT
mNgf-F: TGATCGGCGTACAGGCAGA
mNgf-R: GCTGAAGTTTAGTCCAGTGGG
mMmp3-F: ACATGGAGACTTTGTCCCTTTTG
mMmp3-R: TTGGCTGAGTGGTAGAGTCCC
mLif-F: GCCCCAGAAGTAAAACCTTCAG
mLif-R: CCTTCCATTCTCTCCATTCCAA
mFlt4-F: CTGGCAAATGGTTACTCCATGA
mFlt4-R: ACAACCCGTGTGTCTTCACTG
mCxcl10-F: CCAAGTGCTGCCGTCATTTTC
mCxcl10-R: GGCTCGCAGGGATGATTTCAA
mMmp9-F: CTGGACAGCCAGACACTAAAG
mMmp9-R: CTCGCGGCAAGTCTTCAGAG

Immunofluorescence staining and RNA-FISH

Cultured cells were fixed in 4% paraformaldehyde in PBS for 15 min at room temperature, and blocked for 30 min

in PBS, 3% BSA (Biofroxx, 4240), and 0.3% Triton X-100 (Biosharp, BS084) prior to overnight incubation with primary antibodies. Anti-Sox9 (Cell Signaling Technology, D8G8H), anti-Col2a1 (Bioss Antibodies, bs-10589R), anti-Mmp13 (Bioss Antibodies, bs-10581R) and Collagen10a1 (Biorbyt, orb221376) were used at 1:1000. Cells grown on cover slips for RNA-FISH were fixed in 3.7% formaldehyde solution at room temperature for 10 minutes, then permeabilized with 70% cold ethanol for at least an hour. Stellaris probe was added in 100 μ L of hybridization buffer (Biosearch, Inc.) and incubated in a dark humidified chamber at 37 °C for 4 h. The cells were visualized with DAPI (Sigma, MBD0015) counterstaining (5 ng/mL) under a wide field fluorescence microscope.

Edu incorporation assay

To measure cell growth, 24 hours after transfection in 24-well plates, 20 mM EdU (Ribobio, C10310-1) was added for 8 hour. The cells were then fixed in 3.7% formaldehyde, then washed with PBS and permeabilized. 500 μ L Click-iT reaction cocktail (430 μ L 1xClick-iT reaction buffer, 20 μ L CuSO₄, 1.2 μ L Alexa Fluor[®] azide, and 50 μ L reaction buffer additive) was added to each well and incubated for 45 min at the room temperature in the dark. The cells were counter-stained with DAPI for nuclei and visualized under an inverted fluorescence microscope. Images were processed with Image J and the percentage of EdU incorporation was calculated based on the number of EdU positive (red) and total (DAPI) cells.

Alcian blue staining and quantification

Chondrocytes were cultured for 14 days in chondrogenic differentiation medium, then fixed in 4% formalin for 10 min. After washing twice with PBS, the cells were incubated with 3% acetic acid for 10 min and stained with 1% alcian blue in 3% acetic acid (pH 2.5) for 30 min and photographed. For quantification, the stained cells were washed twice, and the alcian blue dye was extracted with 500 μ L dimethyl sulfoxide (Sigma, D8418). Absorbance was measured at 650 nm.

Alkaline phosphatase assay

Histochemical detection of alkaline phosphatase activity was performed on cells that were fixed for 2 min in 4% paraformaldehyde at room temperature. After washing with TBST, the cells were incubated for 30 min in 0.1 M Tris-HCl, pH 8.5, containing 0.1 mg/ml Naphthol AS-MX phosphate (Sigma, N4875), 0.5% N,N-dimethylformamide (Sigma, D4551), 2 mM MgCl₂, and 0.6 mg/ml fast blue BB salt (Sigma, D9805), and then photographed.

In vitro differentiation of chondrogenic ATDC5 cells

ATDC5 cell line was culture in DMEM/F-12 medium supplemented with 5% FBS, penicillin (100units/mL)/streptomycin (0.1 mg/mL), and 4mM L-Glutamine (Gibco,25030-081). For differentiation experiments, ATDC5 cells were seeded at 80–90% confluence in 12-well plate. After reaching 100% confluence, ATDC5 cells were incubated with serum-free medium for 24 h, then exposed to differentiating medium containing 1% Insulin-transferrin-sodium selenite (ITS, Sigma-Aldrich) and 50nM Vitamin C (Sigma,A4544).

RNA sequencing and data analysis

RNA from Rk5-vector, Full length and DKO mutant *Dnm3os* transfected primary mouse articular chondrocytes were extracted using TRIzol (Life Technologies), followed by purification using a RNeasy Mini Kit (Qiagen,74104). RNA-seq was performed using primary mouse articular chondrocytes from two individual animals. RNA-seq libraries were prepared using the Illumina TruSeq RNA Library Prep Kit v2 and sequenced by a HiSeq 2500 sequencer. RNA-seq reads were aligned to mm10 using TopHat with default settings (.cbcb.umd.edu/).

Statistical analysis

Prism 8.0 (GraphPad software) was employed for analyses. Data from a minimum of three independent experiments were presented as mean \pm s.d. Animals in the experiment were randomly selected and grouped. An unpaired two-tailed Student's t-test was used for analyzing two data sets, and one-way analysis of variance was used for more sets. The significance threshold was set at 0.05 ($p < 0.05$).

Supplementary Information

The online version contains supplementary material available at <https://doi.org/10.1186/s13578-021-00559-8>.

Additional file 1. Clinical description of the proband.

Additional file 2: Fig. S1. Body weight, body length and morphometric characteristics skull in miR-214 KO mice. Body weight (A) and body length (B) of miR-214 KO mice (n=15) and their WT littermates (n = 18) measured starting from 6 week to 24 weeks of age. Body weight and body length of the KO mice were modestly smaller than the WT mice at most time-points examined, the difference was not statistically significant. Morphometric characteristics skull width(C), skull length (D), skull width/length, and inner canthal distance (E) of WT and miR-214 KO, the difference was not statistically significant.

Additional file 3: Fig. S2. miR-214 KO drastically increase the height relative genes. qPCR expression analysis of Noonan syndrome relative genes in miR-214 KO blood, miR-214 Het relative to WT mice (n=5 in each genotype). Data shown are the fold induction of gene expression normalized with Hprt and expressed as mean \pm S.E.M. One-way ANOVA test was used for statistical analysis. ** $P < 0.01$, *** $P < 0.001$, and ns, not significant

Additional file 4: Table S1. Predicted miR-214 and miR-199a recognition sites.

Additional file 5: Fig. S3. LncRNA-Dnm3os impedes chondrocyte differentiation while promotes the proliferation. RT-qPCR quantification of Sox9 in primary articular chondrocytes at passages as noted. (B) RT-qPCR quantification and statistical analysis of *Col1a1* and *Col2a1* in primary articular chondrocytes transfected with sh*Dnm3os* at passages as noted. (C) EdU labeling of proliferating chondrocytes transfected with scrambled shRNA, sh*Dnm3os* and sh*Dnm3os* together with DKO. (D) RT-qPCR quantification of *Dnm3os* in (C). (E) statistical analysis of EdU positive cells in (C). (F) RT-qPCR quantification of *Col10a1* and (G) *Mmp13* in primary articular chondrocytes transfected with scrambled shRNA, sh*Dnm3os* and sh*Dnm3os* together with DKO after 2 weeks chondrocyte differentiation. (H-I) RT-qPCR quantification of overexpression level of *Dnm3os* in primary articular chondrocytes and ATDC5 cells transfected with RK5, FL and DKO. *, $P < 0.05$, **, $P < 0.01$, ***, $P < 0.001$.

Additional file 6: Fig. S4. Forced expression of miR-214 and miR-199a impedes chondrocyte differentiation while promotes the proliferation. Confocal images of GFP and IF staining of *Col2a1* in primary articular chondrocytes after the cells were transfected with P2GM vector, P2GM-miR-199a (P199), or P2GM-miR214 (P214) and differentiated for 2 weeks. (B) RT-qPCR quantification of *Col2a1* or (C) *Col10a1* in cells of (A). (D) the same as in (A) except for the staining of Sox9 and the cells were quantified for Sox9 (E) and (F) *Mmp13* by RT-qPCR. (G) and (H) EdU staining of cells as in (A) and quantification thereof. Student T-test was used for statistical analysis. *, $P < 0.05$, **, $P < 0.01$, ***, $P < 0.001$.

Additional file 7: Fig. S5. Forced expression of *Dnm3os* or *Dnm3os*-DKO downregulates height-related genes in mouse primary articular chondrocytes. RT-qPCR analysis of Noonan syndrome genes in primary chondrocytes that were transfected with pRK5-*Dnm3os* or pRK5-*Dnm3os*-DKO. Data shown are the fold induction normalized against Hprt and are expressed as mean \pm S.E.M. One-way ANOVA test was used for the statistical analysis. ** $P < 0.01$, *** $P < 0.001$, and ns, not significant.

Additional file 8: Fig. S6. Insulin-supplemented differentiation medium cultivation induces differentiation of ATDC5 cells. (A) Alcian blue staining of cartilage matrix produced by differentiated ATDC5 cells after 18-days differentiation. (B-C) RT-qPCR quantifications of *Col1a1*, *Col2a1* in ATDC5 cells at different days of differentiation as noted. (D) RT-qPCR quantifications of *Dnm3os* in ATDC5 cells at different days of differentiation as noted. (E) RT-qPCR quantifications of Sox9 in ATDC5 cells and iMAC cells transfected with RK5, FL and DKO. (G) Top 20 enriched pathways in FL and DKO transfected primary articular chondrocytes. The size and color of the dots represent the enriched gene number and the range of $-\log_{10}(p \text{ values})$, respectively. Student T-test was used for statistical analysis. *, $P < 0.05$, **, $P < 0.01$, ***, $P < 0.001$.

Additional file 9: Table S2. shRNA sequence of *Dnm3os*.

Abbreviations

MAPK: Mitogen-activated protein kinase; ncRNA: Noncoding RNA; lncRNAs: Long non-coding RNAs; NGF: Nerve growth factor; DNM3: Dynamin 3; *Dnm3os*: DNM3 opposite strand; TMJ: Temporomandibular joint; MSCs: Mesenchymal stem cells.

Acknowledgements

We wish to thank the family for participating in this study and other members of the Research Team at Children's Hospitals and Clinics of Minnesota.

Authors' contributions

SY, CL and SYC conceived of the presented idea. TY, QX, SL, HH and LS performed the research. XL and HL contributed to sample preparation and result analysis. SD collected the clinical case and tested the clinical sample. JAR and BAH contributed to the genetic testing and interpreted the results. All authors read and approved the final manuscript.

Funding

This work was supported by grants from the Chinese National Science foundation (81272238, 81261120386, 81672748 and 81871936) to SYC. TTY is supported by a young investigator grant from the Chinese National Science Foundation (81602431). SY is supported by a grant from the Chinese National Science Foundation (81572720). CL is supported by Natural Science Foundation of Jiangsu Province (BK20171053) and National Natural Science Funds of China (81702747).

Availability of data and materials

All data generated or analysed during this study are included in this published article and its additional files.

Ethics approval and consent to participate

The animal study was reviewed and approved by the Institutional Animal Care and Use Committee of Nanjing Medical University.

Consent for publication

Not applicable.

Competing interests

The authors declare that they have no competing interests.

Author details

¹ Department of Medical Genetics, School of Basic Medical Sciences, Nanjing Medical University, Jiangsu 211166 Nanjing, P. R. China. ² Department of Medical Genetics, Children's Hospital and Clinics of Minnesota, Minneapolis, MI 55404, USA. ³ Department of Neurology, Ohio State University Medical Center, Columbus, OH 43210, USA. ⁴ University of Minnesota Medical Center-Fairview, Minneapolis, MI 55404, USA.

Received: 11 October 2020 Accepted: 17 February 2021

Published online: 02 March 2021

References

- Nilsson O, Marino R, De Luca F, et al. Endocrine regulation of the growth plate. *Horm Res*. 2005;64(4):157–65.
- Xing W, Godwin C, Pourteymoor S, et al. Conditional disruption of the osterix gene in chondrocytes during early postnatal growth impairs secondary ossification in the mouse tibial epiphysis. *Bone Res*. 2019;7:24.
- Wit JM, Deeb A, Bin-Abbas B, et al. Achieving optimal short- and long-term responses to paediatric growth hormone therapy. *J Clin Res Pediatr Endocrinol*. 2019;11(4):329–40.
- Jee YH, Baron J. The biology of stature. *J Pediatr*. 2016;173:32–8.
- Baron J, Savendahl L, De Luca F, et al. Short and tall stature: a new paradigm emerges. *Nat Rev Endocrinol*. 2015;11(12):735–46.
- Misra M, Klibanski A. Endocrine consequences of anorexia nervosa. *Lancet Diabetes Endocrinol*. 2014;2(7):581–92.
- Yao B, Wang Q, Liu CF, et al. The SOX9 upstream region prone to chromosomal aberrations causing campomelic dysplasia contains multiple cartilage enhancers. *Nucleic Acids Res*. 2015;43(11):5394–408.
- Stanton LA, Underhill TM, Beier F. MAP kinases in chondrocyte differentiation. *Dev Biol*. 2003;263(2):165–75.
- Jost M, Huggett TM, Kari C, et al. Epidermal growth factor receptor-dependent control of keratinocyte survival and Bcl-xL expression through a MEK-dependent pathway. *J Biol Chem*. 2001;276(9):6320–6.
- Furstenberger G, Senn HJ. Insulin-like growth factors and cancer. *Lancet Oncol*. 2002;3(5):298–302.
- Ornitz DM, Itoh N. The Fibroblast Growth Factor signaling pathway. Wiley Interdiscip Rev Dev Biol. 2015;4(3):215–66.
- Tidyman WE, Rauen KA. The RASopathies: developmental syndromes of Ras/MAPK pathway dysregulation. *Curr Opin Genet Dev*. 2009;19(3):230–6.
- Ling H, Fabbri M, Calin GA. MicroRNAs and other non-coding RNAs as targets for anticancer drug development. *Nat Rev Drug Discov*. 2013;12(11):847–65.
- Burkhardt DD, Rosenfeld JA, Helgeson ML, et al. Distinctive phenotype in 9 patients with deletion of chromosome 1q24-q25. *Am J Med Genet A*. 2011;155A(6):1336–51.
- Descartes M, Hain JZ, Conklin M, et al. Molecular characterization of a patient with an interstitial 1q deletion [del(1)(q24.1q25.3)] and distinctive skeletal abnormalities. *Am J Med Genet A*. 2008;146A(22):2937–43.
- Watanabe T, Sato T, Amano T, et al. Dnm3os, a non-coding RNA, is required for normal growth and skeletal development in mice. *Dev Dyn*. 2008;237(12):3738–48.
- Liu J, Luo XJ, Xiong AW, et al. MicroRNA-214 promotes myogenic differentiation by facilitating exit from mitosis via down-regulation of proto-oncogene N-ras. *J Biol Chem*. 2010;285(34):26599–607.
- Aurora AB, Mahmoud AI, Luo X, et al. MicroRNA-214 protects the mouse heart from ischemic injury by controlling Ca(2+)-overload and cell death. *J Clin Invest*. 2012;122(4):1222–32.
- Huang HJ, Liu J, Hua H, et al. MiR-214 and N-ras regulatory loop suppresses rhabdomyosarcoma cell growth and xenograft tumorigenesis. *Oncotarget*. 2014;5(8):2161–75.
- Loebel DA, Tsoi B, Wong N, et al. A conserved noncoding intronic transcript at the mouse Dnm3 locus. *Genomics*. 2005;85(6):782–9.
- Long F, Ornitz DM. Development of the endochondral skeleton. *Cold Spring Harb Perspect Biol*. 2013;5(1):a008334.
- Gosset M, Berenbaum F, Thirion S, et al. Primary culture and phenotyping of murine chondrocytes. *Nat Protoc*. 2008;3(8):1253–60.
- Lu Z, Lei D, Jiang T, et al. Nerve growth factor from Chinese cobra venom stimulates chondrogenic differentiation of mesenchymal stem cells. *Cell death disease*. 2017;8(5):e2801.
- Li ZZ, Wang F, Liu S, et al. Ablation of PKM2 ameliorated ER stress-induced apoptosis and associated inflammation response in IL-1 β -treated chondrocytes via blocking Rspo2-mediated Wnt/ β -catenin signaling. *J Cell Biochem*. 2020;5:25.
- Bach FC, de Rooij KM, Riemers FM, et al. Hedgehog proteins and parathyroid hormone-related protein are involved in intervertebral disc maturation, degeneration, and calcification. *JOR Spine*. 2019;2(4):e1071.
- Ashraf T, Collinson MN, Fairhurst J, et al. Two further patients with the 1q24 deletion syndrome expand the phenotype: a possible role for the miR199-214 cluster in the skeletal features of the condition. *Am J Med Genet A*. 2015;167A(12):3153–60.
- Desvignes T, Contreras A, Postlethwait JH. Evolution of the miR199-214 cluster and vertebrate skeletal development. *RNA Biol*. 2014;11(4):281–94.

Publisher's note

Springer Nature remains neutral with regard to jurisdictional claims in published maps and institutional affiliations.

Ready to submit your research? Choose BMC and benefit from:

- fast, convenient online submission
- thorough peer review by experienced researchers in your field
- rapid publication on acceptance
- support for research data, including large and complex data types
- gold Open Access which fosters wider collaboration and increased citations
- maximum visibility for your research: over 100M website views per year

At BMC, research is always in progress.

Learn more biomedcentral.com/submissions

